Journal of Pharmaceutical Sciences

MARCH 1977
VOLUME 66 NUMBER 3

RESEARCH ARTICLES

Predictive Conversion of *In Vitro* Drug Dissolution Data into *In Vivo* Drug Response *versus* Time Profiles Exemplified for Plasma Levels of Warfarin

VICTOR F. SMOLEN ˣ **and RANDALL J. ERB**

Abstract □ A mathematical approach to computing the *in vivo* drug response profiles (such as plasma level, pharmacological response, and urinary recovery *versus* time curves) corresponding to observed *in vitro* dissolution of drug dosage form *versus* time profiles is described. The method is exemplified for warfarin tablets, for which observed *in vivo* plasma level profiles are compared to corresponding predicted profiles computed from *in vitro* dissolution data. The potential of the method is demonstrated; approaches to its improvement, as well as its limitations, are discussed.

Keyphrases □ Drug response profiles, *in vivo*—plasma warfarin levels, predicted from *in vitro* dissolution data □ Dissolution data, *in vitro*—predictive conversion into *in vivo* drug response–time profiles, plasma warfarin levels □ Warfarin—plasma levels predicted from *in vitro* dissolution data

Even seemingly trivial changes in the formulation and manufacture of drug products can significantly alter the dynamics of a drug's release from its dosage form and, consequently, affect its therapeutic performance. The growing number of multisource drugs resulting from the expiration of patents is increasing the importance of this problem. It is not feasible to perform routinely the extensive *in vivo* bioavailability testing of drug products necessary to ensure their bioequivalency. Consequently, considerable efforts have been expended to develop and apply *in vitro* drug release tests that are rapid, convenient, and reliable in reflecting the *in vivo* behavior of drug dosage forms. Such tests have to varying degrees been successful in providing results that correlate with *in vivo* bioavailability (1).

Recently, a systematic, control engineering approach to developing drug dissolution tests that are optimally predictive of the entire time course of *in vivo* drug product performance was described (2, 3). Suggestions also were made concerning the manner in which *in vitro* tests may be improved to reflect *in vivo* behavior better (4–6). By properly adjusting the conditions under which drug product dissolution testing is performed, it is sometimes possible to achieve a linear, multiple-point relationship between the time variation of the amount of drug dissolved from dosage forms *in vitro* and analogous amounts absorbed *in vivo* (4); such relationships were successfully demonstrated (7–10). In such cases, it was shown that the time course of *in vivo* pharmacological effects can be computed from *in vitro* dissolution data under certain conditions (4).

Despite such possibilities for handling *in vitro* dissolution data, relationships between the results of *in vitro* drug product dissolution testing and *in vivo* bioavailability are most commonly reported as single-point correlations. For example, the amounts of drug dissolved *in vitro* after a given time are correlated with the amounts absorbed *in vivo* or the plasma levels of the drug observed at the same or other times after dosing (11); times for a percentage of the drug to be dissolved *in vitro* are related to time or rates at which the drug is available *in vivo* (12). It would obviously be of greater utility to correlate or predict the entirety of *in vivo* drug response profiles, *i.e.*, plasma, urinary recovery rate, and/or pharmacological response, *versus* time curves with *in vitro* results and in this manner maximize the amount of information obtainable from drug dissolution testing data.

With drugs such as warfarin, which have a long half-life and are chronically administered, the extent of the drug's bioavailability from its dosage forms is clinically more important than the rates at which it reaches the systemic circulation. However, in addition to not taking full ad-

vantage of all the *in vivo* and *in vitro* kinetic data collected in bioavailability and dissolution experiments, single-point *in vivo* to *in vitro* data correlations can be misinterpreted and misleading as tacit indicators of the extent of drug bioavailability.

For example, in a single-point correlation of average warfarin dissolved from tablets in 1 hr to *in vivo* plasma levels observed after 1 hr (11), a tablet designated A was shown to be approximately 6% dissolved *in vitro* and to elicit a plasma level of 1.11 μg/ml. A second tablet, D, was only about 3% dissolved and yielded a 1-hr plasma level of 0.58 μg/ml. The implication of such linearly correlated results is that Tablet D and other tablets having similar *in vitro* dissolution behavior are only approximately 50% as bioavailable as Tablet A in their dissolution behavior. Actually, however, the areas under the plasma curves reveal Tablet D to have an extent of bioavailability that is 1.08 times that of Tablet A.

This report presents a relatively simple mathematical approach which, under certain described conditions (3, 13, 14), allows the conversion of *in vitro* drug dissolution time curves into *in vivo* drug response *versus* time profiles. The method and its limitations are exemplified using plasma drug levels and dissolution data for warfarin reported by Wagner *et al.* (11).

THEORETICAL

Background and Assumptions—Linear systems theory (15) can be implemented to develop a mathematical relationship which, for a defined set of *in vitro* and *in vivo* experimental conditions, allows *in vitro* drug product dissolution *versus* time data to be transformed into computationally predicted or simulated *in vivo* drug response *versus* time profiles. This is feasible to accomplish provided that the dynamics of the system behavior can be presumed linear, *i.e.*, the following assumptions and conditions apply:

1. The *in vitro* and *in vivo* kinetic processes remain qualitatively the same for all of the different dosage formulations tested.

2. All kinetic processes can be described as linear, or at least approximated as linear, in the sense that the superposition principle (16) applies over an operational range of interest. *In vivo*, both the preabsorption dynamics of the drug's release from its dosage forms and the subsequent systemic absorption into the blood, as well as its disposition and elimination from the body, are required to be dose independent and nonsaturable, *i.e.*, linear. In practice, it may be sufficient that the *in vivo* system approximates linearity over the range of difference seen between the dosage forms tested. However, as commonly heard, it is not necessary that the *in vivo* bioavailability of the drug be rate limited only by its dissolution from its dosage forms. However, the *in vivo* absorption, as well as any presystemic metabolism of the drug in the gut lumen, wall, or liver, must be linear and describable by proportional rate constants that are time invariant. In other words, drug absorption occurring by site specific, facilitated, or active transport, as well as the involvement of saturable metabolic processes, could vitiate the approach, depending upon the magnitude of the effects.

It is emphasized, however, that the *in vitro* time course of dissolution rates or extents of release of the drug from its dosage form can theoretically have any type of kinetic behavior provided that the apparatus and conditions of the *in vitro* dissolution test are such that the experimentally recorded drug dissolution rate or extent *versus* time profiles are direct reflections of drug release into the dissolution media or are consistently related to it by first- or higher order lag times (transfer function) (13). However, in the extreme case where a drug dissolves so slowly that its dissolution time exceeds its transit time in the GI tract, *in vitro* dissolution curves that are run to completion will obviously predict a greater *in vivo* bioavailability than would actually be observed; conceivably, this result could be at least approximately corrected for by truncating *in vitro* dissolution experiments after a time *in vitro* that is known to exceed a correspondingly proportional time *in vivo* at which further absorption of the drug no longer proceeds. The other extreme of instantaneous drug release, as is accomplished by administering a solution of the drug, merely represents an impulse input to the GI contents (2, 13, 14) and poses no theoretical difficulties.

3. No specific chemical or biochemical effects are operative with any dosage form being tested that are not operative with the rest. The operation of such biologically specific factors can be introduced if the drug forms soluble, nonabsorbable complexes with excipients in the formulations or if such excipients alter the barrier properties of the GI mucosa through which the drug must pass to be systemically absorbed. Such biological occurrences obviously could not be easily detected or taken into account by *in vitro* testing results unless they consistently occurred in all dosage forms (3).

General Computational Procedure—With the described assumptions and limitations in mind, the application of linear systems, transfer function, analysis provides the mathematical means to relate and predict *in vivo* drug response profiles, symbolized as $Q_B(t)$, from *in vitro* dissolution rate *versus* time profiles, presently symbolized as $\dot{A}(t)_D$, once a weighting function, $G_{BD}(t)$ [or transfer function, $G_{BD}(s)$, as defined in the complex frequency domain] is established. A function, f, is converted from the time domain, $f(t)$, into the complex frequency domain, $F(s)$, by taking its Laplace transform, as defined by:

$$F(s) = \int_0^\infty f(t)e^{-st}\,dt \qquad \text{(Eq. 1)}$$

The advantage of working in the s domain relative to the time, t, domain, is that the mathematical operations of convolution and deconvolution necessary in the time domain to compute output functions from input functions and vice versa are replaced by multiplication and division, respectively. For the present purposes, there are two such input–output transfer function relationships to consider, one for the *in vitro* system and another for the *in vivo* system. The *in vivo* response to an oral dosage form would be given by Eq. 2:

$$Q_B(s) = G_B(s)\dot{A}(s)_G \qquad \text{(Eq. 2)}$$

where $\dot{A}(s)_G$ is the Laplace transform of the time curve which describes the *in vivo* rate of drug release into the GI contents and, therefore, represents the *in vivo* input function (14); $\dot{A}(s)_G$ has an *in vitro* counterpart, $\dot{A}(s)_D$, which describes the rates of dissolution *in vitro*. For example, $\dot{A}(s)_D$ for a flow-through dissolution apparatus (3) would be given by Eq. 3:

$$\dot{A}(s)_D = \dot{V}C(s) \qquad \text{(Eq. 3)}$$

where $\dot{V}(t)$ is the flow rate through the dissolution cell, and $C(t)$ is the concentration in the stream; $C(t)$ can be continuously monitored using a spectrophotometer equipped with a flowcell. The flow rate is usually kept constant.

The transfer function for a linear system(s) that is generally applicable to relating *any* input is defined and obtained in the Laplace domain as the ratio of any *known* output function from the system to the corresponding *known* input function that caused the output. If $\dot{A}(s)_{G,r}$ and $\dot{A}(s)_{D,r}$ are known for any reference dosage form, r, for which the assumptions of linearity apply to both the *in vivo* and *in vitro* systems, they can be considered as input and output functions, respectively, and interrelated by the transfer function defined by:

$$\frac{\dot{A}(s)_{G,r}}{\dot{A}(s)_{D,r}} = G(s)_{DG,r} \qquad \text{(Eq. 4)}$$

Once $G(s)_{DG,r}$ is known, it can be used to compute *in vivo* response profiles, $Q_B(s)_i$, for any ith dosage form using *in vitro* determined dissolution input functions and:

$$Q_B(s)_i = G(s)_B G(s)_{DG}\dot{A}(s)_{D,i} \qquad \text{(Eq. 5)}$$

In practice, it is computationally expeditious to treat *in vitro* dissolution data as the output, $Q_D(s)$, relating it directly to the *in vivo* output, as shown in Eq. 6:

$$\frac{Q_B(s)_r}{Q_D(s)_r} = G(s)_{BD,r} \qquad \text{(Eq. 6)}$$

This equation defines a transfer function, $G(s)_{BD,r}$, based upon data from a reference dosage form, r.

For any other dosage forms that do not violate the assumptions on which this treatment is based, the *in vivo* response profile will be given by Eq. 7 using the *in vitro* dissolution data results observed for the ith dosage form:

$$Q_B(s)_i = G(s)_{BD,r}Q_D(s)_i \qquad \text{(Eq. 7)}$$

The two approaches obviously yield the same results. The relationship between *in vitro* dissolution and *in vivo* absorption dynamics is now

implicit in $G(s)_{BD,r}$. The conditions of the *in vitro* test must, of course, be maintained while testing each dosage form. Obviously, if the dissolution test does not yield at least some type of single-point correlations, such as between the time for 50% of the drug to dissolve *in vitro* and the time for 50% of the drug to be absorbed *in vivo*, it probably cannot provide results from which entire plasma levels, urinary recovery rates, and/or pharmacological response *versus* time profiles can be predicted.

The computational operations of deconvolution (Eq. 6) and convolution (Eq. 7) can be performed by various methods. Some methods used in pharmacokinetics were described previously (13, 14, 17, 18), and all of the various techniques generally used in engineering practice were recently reviewed (17). Such computations may rapidly and conveniently be performed using a Fourier analyzer[1] computer, as was implemented to obtain the results described in the present report. However, such specialized equipment is expensive and not very common. Therefore, a computational scheme for convolution–deconvolution appropriate for analog computers is presented in the *Appendix*. The same results are obtainable from the analog computer approach, which is presented here merely as a convenience to investigators without access to a Fourier analyzer.

EXPERIMENTAL

***In Vitro* Dissolution and *In Vivo* Plasma Curve Data**—The *in vitro* and *in vivo* data for warfarin treated in this study were abstracted from a report by Wagner *et al.* (11). Four dose treatments using four different dosage forms (Tablets A[2], B[3], C[4], and D[5]) were studied by these authors. Panels of six and 12 human volunteers were used in two separate studies. In the first study, six subjects received 25-mg dose treatments of Tablet B. In the second study, 12 subjects received 10-mg doses of Tablets A, C, and D. Plasma samples were periodically collected from the volunteers and assayed for the drug.

Dissolution testing of the tablets was performed using a paddle-agitated, three-necked, round-bottom flask, in which individual tablets were initially exposed to 900 ml of 0.1 *N* HCl for 30 min followed by the addition of 100 ml of strong phosphate buffer. The buffer instantaneously raised the pH to 7.5 ± 0.1 for the remainder of the dissolution test. The amounts of warfarin dissolved from the tablets as a function of time were determined by circulating the dissolution medium through a flowcell in a spectrophotometer. The tablets used were reported to have been assayed for their drug content using the official USP XVIII method.

Data Treatment—The average data reported by Wagner *et al.* (11) for each dose treatment were used to perform the described computations. Tablet C, administered as two 5-mg tablets, was selected as the reference dosage form from which data were used to determine the *in vitro* input → *in vivo* output transfer function, $G(s)_{DB,r}$; $G(s)_{DB,r}$ was subsequently used to compute plasma level *versus* time profiles for Tablets A (two 5-mg tablets), D (two 5-mg tablets), and B (one 25-mg tablet).

To obtain data points at discrete, constant time intervals, as needed for subsequent convolution and deconvolution computations, the *in vivo* plasma level data for Tablet B were fitted to multiexponential expressions of the form $y = \Sigma_{i=1}^{n} A_i e^{-m_i t}$. An iteratively converging, least-squares, digital computer program, which performs log peeling and derives initial estimates for the equation parameters (A_i's and m_i's), was used to perform the fitting. This program, called MULTIFIT, was developed in this laboratory (19). By using the fitted equations, data points were interpolatively generated at 2-hr intervals for up to 96 hr.

The *in vitro* dissolution test data, reported as cumulative amounts of drug dissolved *versus* time profiles, were incomplete in that the testing was prematurely discontinued before all of the drug in the tablets was dissolved. Consequently, an equation of the form $Q_D(t)_\% = 100\,(1 - e^{-kt})$, where $Q_D(t)_\%$ is the percent of the drug dissolved at time t, was fitted by linear least-squares regression to the data reported by Wagner *et al.* (11); the symbol k represents an apparent first-order dissolution rate constant.

This curve fitting was performed to allow the extrapolation of the *in vitro* dissolution curves to 100% to account for all of the drug contained in the tablets; values generated by the fitted equations were only used to obtain data points lying beyond the times at which the experimental data were truncated. Before these times, the *in vitro* data were directly estimated at 5-min intervals from the dissolution curves reported previously (11).

Convolution—The convolution and deconvolution computations were made with the use of a Fourier analyzer[1]. The system performs discrete Fourier transformation of time data and arithmetical operations on functions in the frequency domain. The Fourier transform of a time function as defined by Eq. 8 has similar properties to its Laplace transform:

$$\mathcal{F}f(t) = \int_0^\infty f(t)e^{-j\omega t}\,dt \qquad \text{(Eq. 8)}$$

$$\mathcal{F}f(t) = F(\omega) \qquad \text{(Eq. 9)}$$

In Eqs. 8 and 9, $j = \sqrt{-1}$ and ω is frequency. In the Laplace complex frequency domain, transformation of time functions yields, instead of ω, functions of a complex number, $s = \sigma + j\omega$. The σ is a real part added as a convergence factor; it allows transformation of some functions that otherwise cannot be Fourier transformed (20). For present purposes, the use of Fourier transforms can be considered equivalent to Laplace transforms. The Fourier analyzer-computer system obtains discrete finite transforms of time data using the algorithm defined by:

$$f(m\,\Delta f) = \Delta t \sum_{N=0}^{N-1} f(n\,\Delta t)e^{-j2\pi mn\,\Delta\omega\,\Delta t} \qquad \text{(Eq. 10)}$$

where Δt is the time interval between data points, $f(n\,\Delta t)$ is the measured value of the data point, ω is the frequency in Hertz, N is the number of data points, and m and n are integers denoting the multiple discrete time and frequency values.

The computations were performed on the Fourier analyzer using a data block size of 256 channels. The Fourier transform of the *in vivo* data was taken using data points at 2-hr intervals for up to 96 hr. *In vitro* data points were spaced 5 min apart for up to 1280 min. The transfer function, $G(s)_{DB,r}$ [more accurately symbolized as $G(\omega)_{DB,r}$] was obtained for Tablet C data by complex division in the frequency domain as the ratio $Q_B(\omega)_c/Q_D(\omega)_c$. Fourier-transformed *in vitro* data for any particular tablet was then multiplied by the transfer function, $G(\omega)_{DB,c}$, to obtain the Fourier transform of the *in vivo* plasma level curve which was to be computationally predicted for that tablet. The result was then multiplied by a scale factor which appropriately adjusted the gain of the transfer function as needed in accordance with the actual assayed amount of drug contained in the tablet(s). The inverse Fourier transform of this result then provided the computational prediction of the *in vivo* plasma drug level *versus* time profiles for the dosage form.

The scale factor (*SF*) for dose treatments with Tablet A was 9.88 mg/8.9 mg = 1.02; for Tablet D, the *SF* was 9.40 mg/8.94 mg = 1.05; for Tablet B, the *SF* was 23.9 mg/8.94 mg = 2.67. The *SF* values are calculated using reported assay results (11) for drug content in the tablets rather than with nominal values. The *SF* values are needed to normalize the transfer function first to unit, 1-mg, doses of the drug and then to adjust the magnitude of each $Q(t)_{D,i}$ to correspond to the actual amount of drug input to the system.

The computational steps followed to convert *in vitro* drug dissolution curves into their corresponding plasma level curves are summarized in Scheme I.

$$\text{Step 1: } Q_B(t)_r \xrightarrow{\text{FT}} Q_B(\omega)_r$$

$$\text{Step 2: } Q_D(t)_r \xrightarrow{\text{FT}} Q_D(\omega)_r$$

$$\text{Step 3: } Q_D(t)_i \xrightarrow{\text{FT}} Q_D(\omega)_i$$

$$\text{Step 4: } Q_B(\omega)_i = \frac{Q_B(\omega)_r}{Q_D(\omega)_r} Q_D(\omega)_i SF = G_{DB}(\omega)Q(\omega)_i SF$$

$$\text{Step 5: } Q_B(\omega)_i \xrightarrow{\text{IFT}} Q_B(t)_i$$

Scheme I—Summary of stepwise computational procedure implemented on a Fourier analyzer to obtain the conversion of in vitro *drug product dissolution curves into* in vivo *plasma level curves. The subscript* r *corresponds to the reference dosage form from which the transfer function is obtained. FT and IFT refer to Fourier and inverse Fourier transformations, respectively.* $Q_B(t)_i$ *and* $Q_D(t)_i$ *symbolize biological response and dissolution profiles for an* ith *dosage form, and* $Q_B(\omega)_i$ *and* $Q_D(\omega)_i$ *refer to their Fourier transforms.*

[1] Hewlett-Packard 5451B, Santa Clara, Calif.
[2] Coumadin sodium, 5 mg, Endo Laboratories.
[3] Coumadin sodium, 25 mg, Endo Laboratories.
[4] Athrombin-K, 5 mg, Purdue Frederick.
[5] Panwarfin sodium, 5 mg, Abbott Laboratories.

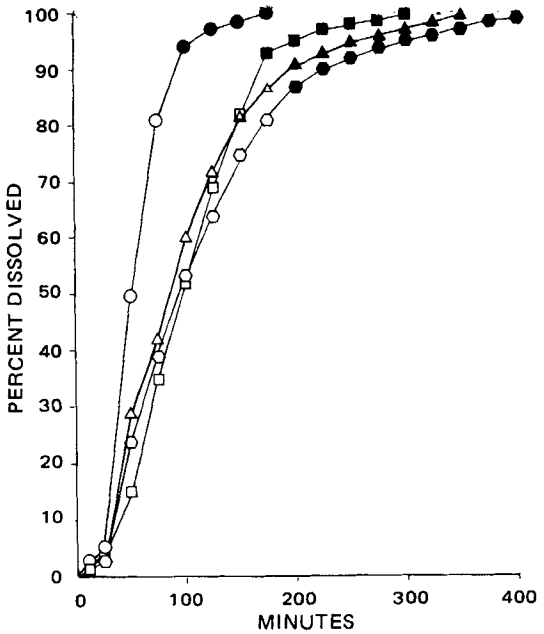

Figure 1—In vitro *dissolution curves plotted as percent warfarin dissolved for Tablets A (○), B (□), C (△), and D (○). Extrapolated values (●, ■, ▲, and ●), indicated on the latter part of the curves, resulted from fitting the earlier observed points to the equation* $Q_D(t)_c = 100(1 - e^{-kt})$, *where* $Q_D(t)_c$ *is the percent drug dissolved and K is a constant.*

RESULTS

Exponential Curve Fitting to *In Vitro* and *In Vivo* Data—Figure 1 presents the linear least-squares fits of the *in vitro* dissolution data results reported by Wagner *et al.* (11) to curves described by the equation $Q_D(t)_\infty = 100(1 - e^{-kt})$. The early observed data points on the time curve, indicated by the open symbols, were used to obtain a least-squares value for the apparent first-order dissolution rate constant, k, by fitting them to a linearized form of the equation given by $\log_e[1 - Q_D(t)_\infty/100] - kt$, where $Q_D(t)$ is the percent of the drug dissolved at any time, t. Linear correlation coefficients for comparisons of data points computed from the fitted equation with corresponding observed values were 0.96, 0.95, 0.98, and 0.99 for Tablets A, B, C, and D, respectively. Therefore, the assumed first-order dissolution of the tablets described by the fitted equations was satisfactory and could be used to estimate data points extrapolatively for dissolution curves beyond the times at which the dissolution tests were prematurely terminated. The solid symbols in Fig. 1 represent such values estimated with the use of the fitted equations.

The curve in Fig. 2 is a plot of the least-squares multiexponential fit obtained to the *in vivo* plasma level data observed for Tablet C. The data

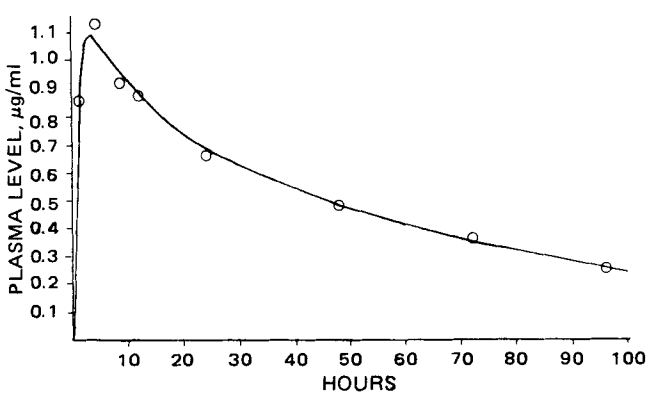

Figure 2—*Time variation of averaged plasma warfarin levels observed following dosing of 12 human subjects with two 5-mg tablets (Tablet C). The convolution of this curve with the* in vitro *dissolution profile shown in Fig. 1 for Tablet C provided the weighting function,* $G_{DB}(t)_c$ *(shown in Fig. 3), used for the computational prediction of plasma curves from* in vitro *data.*

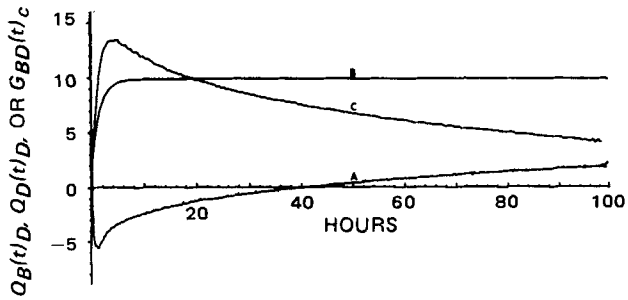

Figure 3—*Computer-constructed time curves exemplifying the functions used to predict* in vivo *plasma curves computationally from* in vitro *dissolution data for Tablet D. Curve A represents the weighting function,* $G_{BD}(t)_c$, *derived from the deconvolution of the* in vitro *dissolution profile,* $Q_D(t)_c$ *(percent dissolved), with the observed* in vivo *plasma curve,* $Q_B(t)_c$ *(micrograms per milliliter), for the reference dosage form, C.* $G_{BD}(t)_c$ *was convolved with the* in vitro *dissolution profile,* $Q_D(t)_D$ *(curve B, with the ordinate* $\times 10^{-1}$*), to obtain the computationally predicted plasma curve,* $Q_B(t)_D$ *(curve C, with the ordinate* $\times 10^{-1}$*).*

were abstracted from Wagner *et al.* (11). The equation for the curve is given by:

$$Q_B(t)_c = 0.91e^{-0.0133t} + 0.36e^{-0.1200t} - 1.27e^{-1.261t} \quad \text{(Eq. 11)}$$

The sum of squares of deviations from the fitted curve is 0.04917. The curve provides a satisfactory representation of the observed data points.

Comparisons of Computed and Observed Plasma Curves—As already discussed, the Fourier transforms of the curve in Fig. 2 and the dissolution curve for Tablet C in Fig. 1 were deconvolved to provide the transfer function, $G_{DB}(\omega)_c$. A computer-constructed plot of the resulting inverse Fourier transform of $G_{DB}(\omega)_c$, *i.e.*, the weighting function $G_{DB}(t)_c$, is presented in Fig. 3. Mathematically, a weighting function is usually defined as the transient time response of a system to an impulse, *i.e.*, Dirac delta function (21) input. However, as a consequence of defining the cumulative warfarin dissolution profiles, $Q_D(t)_i$ [rather than using rates of dissolution, $\dot{Q}_D(t)_i$] as the inputs into the hypothetical linear system that converts *in vitro* data into *in vivo* plasma curves, the weighting function in this case is the derivative of the impulse response, *i.e.*, the doublet response (21). This fact accounts for its values being negative and lying in the fourth quadrant.

The cumulative drug dissolution profiles were chosen as the input function in order to use data for the predictive computations that were as close to those that were experimentally observed as possible. Exemplary results for Tablet D are also shown in Fig. 3, which presents a comparison of the forms of $G_{DB}(t)_c$ with $Q_D(t)_D$ (curve B) with which it is convolved to obtain the computationally predicted plasma curve, $Q_B(t)_D$, for Tablet D (curve C).

The transfer function, $G_{DB}(\omega)_c$, was consistently employed (Scheme I) to obtain the computationally predicted *in vivo* plasma curves for Tablet A (10-mg), D (10-mg), and B (25-mg) dose treatments shown in Figs. 4, 5, and 6, respectively. The computed plasma curves can be directly

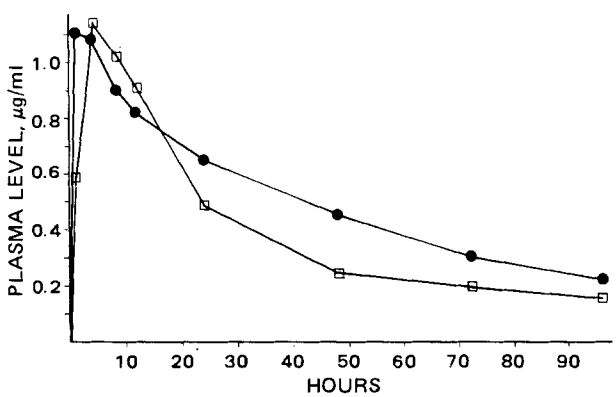

Figure 4—*Comparison of a computationally predicted (□) plasma warfarin curve for Tablet A (two 5 mg), calculated from the results of* in vitro *drug dissolution testing, with the average plasma curve (●) observed in an* in vivo *study of 12 human subjects (11).*

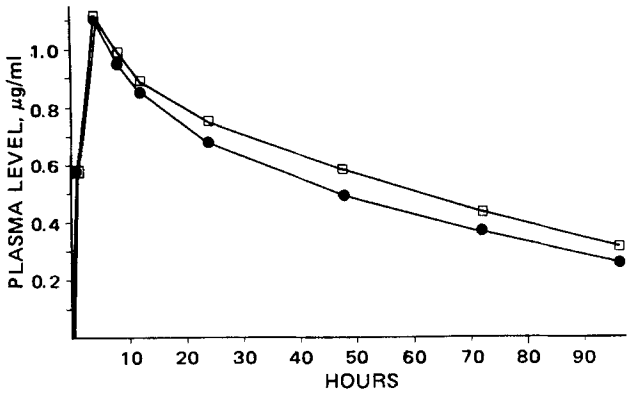

Figure 5—*Comparison of a computationally predicted* (□) *plasma warfarin curve for Tablet D (two 5 mg), calculated from the results of* in vitro *dissolution testing, with the average plasma curve* (●) *observed in an* in vivo *study of 12 human subjects (11).*

compared to the *in vivo* observed average curves, which are in each case plotted on the same coordinates.

Figure 6 contains an additional curve resulting from a correction of the computed curve for the incomplete absorption of only 84% of the administered dose. The corrected curve more closely resembles the observed data points. Without the *a priori* knowledge that the extent of warfarin bioavailability from Tablet B is only 84% of that obtained from Tablet C, the computed plasma curve obviously overestimates the *in vivo* drug absorption efficiency of Tablet B. In each case, as shown in Figs. 4–6, the points plotted on the predicted plasma curves were computed from the results of the convolutions at the same time at which blood sampling was performed *in vivo*; this procedure allowed a direct comparison of each computationally predicted point with its *in vivo* observed counterpart.

The results of plotting each observed plasma level data point as a function of its *in vitro*, computationally predicted, counterpart are shown in Fig. 7. The straight line in Fig. 7 is drawn through the origin with a slope of unity. If the data were exact and the correspondence between the *in vivo* and *in vitro* predicted data points was perfect, all points plotted in Fig. 7 would obviously fall exactly on this line. The largest discrepancies are seen at the upper end of the line for Tablet B for which *in vitro* predicted data points left uncorrected for incomplete *in vivo* absorption were used in constructing the plot.

The relatively excellent linear correlations of the *in vitro* predicted and *in vivo* observed data seen in Fig. 7 can be contrasted to the comparatively poor linear relationship seen between the *in vitro* and *in vivo* data plotted in Fig. 8. In this case, the *in vivo* plasma levels observed for each dosage form were merely plotted as a function of the corresponding rates of percent dissolved *in vitro* [*i.e.*, $\dot{Q}_D(t)_{\%,i}$] occurring at times ap-

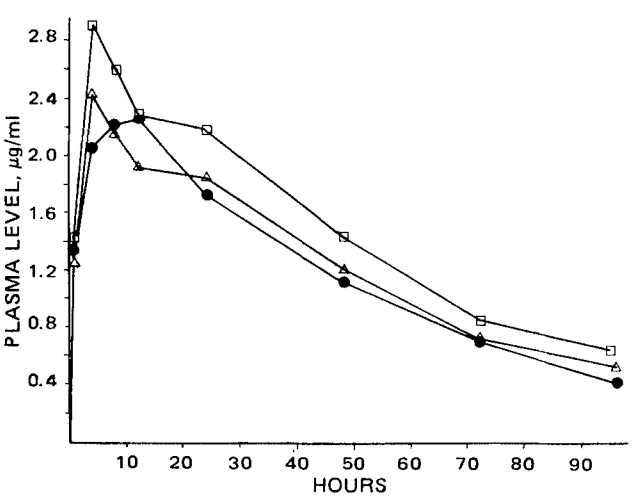

Figure 6—*Comparisons of computationally predicted* [*uncorrected* (□) *and corrected* (△) *for an incomplete, 84%,* in vivo *absorption*] *plasma warfarin curves for Tablet B (one 25 mg), calculated from the results of* in vitro *drug dissolution testing, with the average plasma curve* (●) *observed in an* in vivo *study of six human subjects (11).*

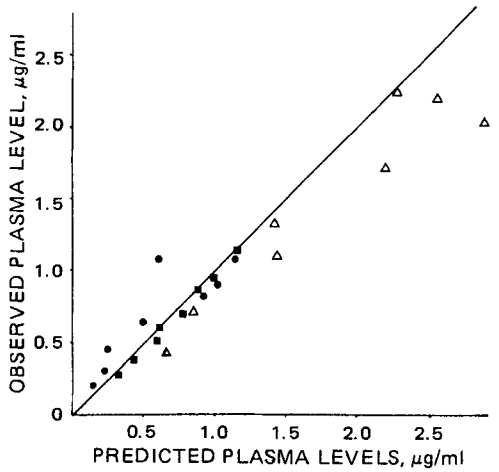

Figure 7—*Linear plot comparison of computationally predicted plasma warfarin levels for Tablets A (two 5 mg,* ●), *B (one 25 mg,* △), *and D (two 5 mg,* ■) *with plasma levels observed at corresponding times in an* in vivo *study (11). The computations were made using data from the same panel of 12 subjects used to study Tablets A and D; data for B were obtained in another study with six human volunteers.*

propriately scaled to correspond to the *in vivo* plasma curves. The scale factor of $\frac{1}{15}$ aligns the *in vitro* and *in vivo* curves on the time axis and is based on the relative times for dissolution to be virtually completed as compared to the return of plasma drug levels to zero; the relative time scales involved can be seen in Fig. 3 for the plot of $Q_D(t)_D$ and $Q_B(t)_D$, respectively.

The $Q_D(t)_i$ values at each time corresponding to an observed plasma level were calculated using the derivative of the equations providing the linear least-squares fits to the *in vitro* drug dissolution profiles shown in Fig. 1; *i.e.*, the values were obtained from $Q_D(t)_{\%,i} = 100k_i e^{-k_i t/15}$, where k_i is the least-squares, apparent dissolution rate constant for the ith dosage form. As was the case in Fig. 7, the straight line in Fig. 8 is again drawn through the origin with a slope of unity. The systematic deviations of the points from this line are quite apparent.

The linear correlations of *in vitro* predicted to *in vivo* observed plasma levels shown in Fig. 6 are summarily described in Table I. The Pearson, r, linear regression coefficients indicate that the calculated plasma level curves are highly correlated with the actual *in vivo* observed plasma levels. A perfect correspondence between computed and observed plasma levels would provide least-squares values of 1.00 for the slopes, zero for the intercepts, and 1.00 for the linear regression coefficients. The ratios of the areas under the calculated and observed plasma curves are also

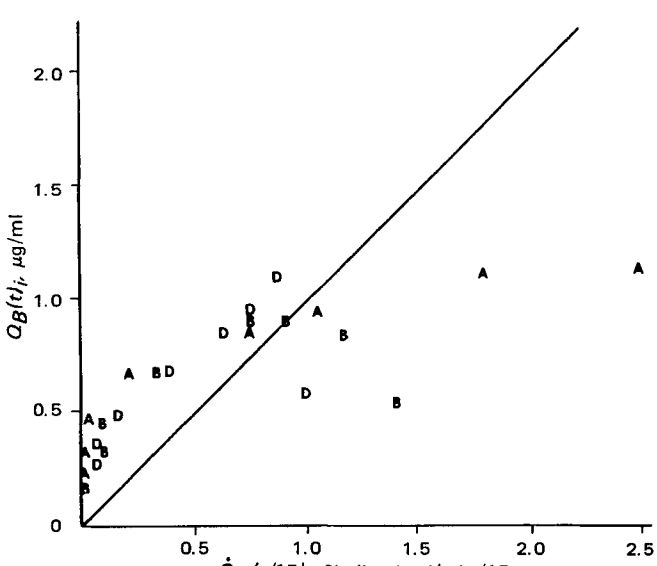

Figure 8—*Linear plot comparison of* in vitro *dissolution rates,* $Q_D(t/15)_i$, *for Tablets A (two 5 mg), D (two 5 mg), and B (one 25 mg) to corresponding* in vivo *observed plasma levels,* $Q_B(t)_i$. *(See text.)*

Table I—Results of Comparisons of Plasma Warfarin Levels for Different Dose Treatments, which were Computationally Predicted from *In Vitro* Dissolution Data with Corresponding *In Vivo* Observed Plasma Levels

Dose Treatment	Statistical Parameters[a]				
	a^a	b^a	r^b	p^b	Computed AUC^c / Observed AUC
Tablet A (10 mg)	0.74	0.26	0.85	0.01	0.79
Tablet D (10 mg)	1.04	−0.08	0.99	0.001	1.11
Tablet B (25 mg)	0.80	0.05	0.95	0.001	1.23
Tablet B (25 mg) X 0.84	0.96	0.03	0.95	0.001	1.04

[a] Linear regression line of best fit: $y = ax + b$. [b] Pearson r, the linear least-squares regression coefficient, and its probability level, p, for the computationally predicted *in vivo* plasma levels compared to corresponding observed *in vivo* plasma levels. [c] Ratios of the areas under the *in vivo* curves (AUC) from 0 to 90 hr for the computed and actual plasma levels.

listed in Table I to provide an indication of the fidelity with which the computations can predict the extent of drug bioavailability from the tablets.

DISCUSSION

A comparison of the two types of linear correlations (Figs. 7 and 8) of *in vitro* data derived from dissolution testing with *in vivo* plasma levels clearly justifies the added computational effort required to obtain computationally predicted plasma curves in assessing the bioavailability behavior of drug dosage forms from *in vitro* studies. Figure 8 was constructed using *in vitro* dissolution rates that proceed through a maximum and decay with time in a manner analogous to plasma level curves, which they obviously resemble much more than cumulative amount *versus* time curves; the latter proceed to a plateau at 100% dissolved. Because of their at least superficial resemblance to plasma curves, dissolution rates rather than extents were chosen for the correlations to make them appear as good as possible and comparable to those in Fig. 7.

As expected, and as confirmed by Fig. 8, multiple-point correlations of dissolution rates with plasma levels are obviously nonlinear. This is the case even when the dissolution rates are properly time scaled. Therefore, the direct use of *in vitro* dissolution data provide, at least in the present case for warfarin, a poor predictor of *in vivo* drug product performance. In contrast, the use of *in vitro* predicted plasma levels obtained by the computational conversion of observed *in vitro* dissolution data provides a theoretically rational, meaningful, and more reliable means of judging the *in vivo* behavior of drug products from the results of *in vitro* dissolution testing. However, the limitations of even this method, as exemplified by the discrepancies in Table I, must be kept in mind.

Deviations of predicted from observed *in vivo* results can be attributed to violations of any or all of the assumptions on which the linear systems treatment of the data is based. Unfortunately, linear systems theory provides the only generally applicable means of converting *in vitro* dissolution profiles into predicted *in vivo* drug response profiles. Any attempts to improve the relationships through the use of nonlinear modeling approaches require some knowledge of the specific mechanisms operating in any given case to produce the observed or suspected nonlinear systems behavior. Such information is commonly unavailable. If it were available, its applicability to any particular drug formulation might not be known *a priori*; consequently, its usefulness in predicting *in vivo* bioavailability behavior would be vitiated. Therefore, despite its shortcomings, the presently implemented linear systems method of computationally predicting *in vivo* drug performance represents the best, generally applicable, approach to converting *in vitro* data into *in vivo* drug response profiles that is likely to be devised.

Considering the many assumptions involved in the linear systems, transfer function, approach applied in this study, the predictions obtained are quite good and generally fall close to the observed *in vivo* data. The results (Figs. 4–6) are quite successful in predicting two out of three of the plasma level curves for the drug from *in vitro* dissolution profiles. Direct comparisons of the data points obtained from computationally predicted plasma profiles with their corresponding experimentally observed *in vivo* plasma curves in all cases provided linear correlation probabilities of $p \geq 0.01$ or 0.001 (Table I), indicating that the shapes of the computed and *in vivo* plasma curves over time were nearly the same.

As expected, however, differences in the extent of *in vivo* bioavailability cannot always be predicted, as was the case for Tablet B. This treatment, relative to the others, was only 84% bioavailable, even though its dissolution *versus* time profile was well within the range reported for the other tablets. This particular discrepancy may at least in part be attributable to the *in vivo* data for Tablet B having been obtained from a separate study involving a panel of six subjects whereas the other *in vivo* data came from a different panel of 12 subjects. Treatment B also consisted of a single 25-mg tablet as opposed to the other dose treatments being comprised of 10-mg doses (two 5-mg tablets). In any event, results obtained for Tablet B exemplify a limitation of all *in vitro* dissolution testing in being incapable of predicting exceptions to previously observed correlations. Although this limitation may be minimized by judiciously selecting the design of the dissolution apparatus and systematically optimizing the process conditions of the dissolution testing (3), it cannot be always entirely eliminated.

As demonstrated by the results of the present study, the *in vitro* computational predictions of *in vivo* bioavailability may be expected to have the greatest fidelity for dosage formulations that are the most similar to the reference dosage form from which the transfer function is obtained. Therefore, for dosage formulations with the same nominal dose content and of qualitatively equal composition, predictions of the *in vivo* drug response profile for the same panel of subjects from which the *in vivo* data for the reference dosage form were obtained can probably be made with an often acceptable degree of fidelity. This would particularly be the case in quality control testing for *in vivo* significance of batch-to-batch variations. Obviously, in all cases, consistency in the process variables of the test, such as the geometry of the apparatus, the dissolution medium composition, and agitation, must be maintained. Ideally, dissolution testing should be performed with a flexible method using process variables that have been systematically optimized to provide directly drug dissolution profiles that are predictive, within predetermined confidence levels, of *in vivo* drug response profiles (3). A new control engineering approach to accomplish such systematic optimization of drug dissolution testing methodologies was described previously (3).

Although optimized dissolution testing methods are always to be preferred, the predictive estimates of *in vivo* drug product performance obtained by the methods and apparatus commonly used (20) may conceivably be improved and expanded through the incorporation of data from an increasing number of dosage formulations into the transfer function as such additional data become available. For this purpose, the *in vitro* data must always be obtained using the same dissolution test conditions; however, *in vivo* data would generally be obtained with different panels of human subjects. The simplest approach would be to combine transfer functions obtained for different drug formulations into an average.

For example, in the present case, an average transfer function obtained for Tablets A, C, and D, *i.e.*, $\overline{G}_{DB}(s)_{A,C,D}$, would likely improve the prediction of plasma level curves for other dose treatments resembling A, C, and D. However, each individual, $G_{DB}(s)_i$, transfer function could not be expected to produce predictions with equal fidelity. Therefore, it is reasonable to weight the contribution of each individual transfer function on the basis of its predictive capability. Such a weighted average transfer function for different formulations could be defined by Eq. 12:

$$\overline{G}_{DB}(s) = \sum_{i=1}^{N} W_i G_{DB}(s)_i \qquad \text{(Eq. 12)}$$

where $W_i (\Sigma_{i=i}^{N} W_i = 1)$ represents the weight factors for the transfer functions derived from data observed for each ith drug formulation.

A weighting scheme that might be used to obtain W_i values could be based on the ability of the ith transfer function to predict the plasma curves observed for the other $N - 1$ dosage forms contributing to the average, as expressed by:

$$W_i = \frac{\sum_{J=1 \neq i}^{N-1} \sum_{q=1}^{K} (P_{\text{pred}} - P_{\text{obs}})_q^{-2}}{\sum_{i=1}^{N} \sum_{J=1 \neq i}^{N-1} \sum_{q=1}^{K} (P_{\text{pred}} - P_{\text{obs}})_q^{-2}} \qquad \text{(Eq. 13)}$$

where P_{pred} and P_{obs} represent computationally predicted and observed data points corresponding to the qth sampling time, respectively; and K is the total number of data points sampled for the ith dosage form. The W_i defined by Eq. 13 emphasizes the predictive capability of each $G_{DB}(s)_i$. Weighting for variability of the *in vivo* data for each dosage form contributing to the average transfer function is attenuated by the predictive capability of the transfer function and is, therefore, implicit in

the value of each W_i. By using this scheme or some alternative one, transfer functions for predicting *in vivo* temporal drug response behavior could be continuously updated as new data from additional dosage forms become available.

SUMMARY AND CONCLUSIONS

Single-point correlations of *in vitro* drug dissolution behavior with *in vivo* bioavailability results for different drug dosage forms do not take advantage of all of the observed data and can have serious shortcomings with regard to their significance and interpretation. Therefore, a mathematical, linear systems, approach to computationally predicting *in vivo* drug response *versus* time curves [such as plasma levels, pharmacological responses (22), and urinary recovery rates] from observed *in vitro* drug product dissolution time curves was developed and exemplified with data for four different dosage forms of warfarin (11).

Despite the linearity assumption implicit in the use of the approach, the method was verified by the surprisingly good computational predictions of *in vivo* plasma curves, which were produced for two of the dosage forms (A and D). The discrepancy observed for a third dosage form was in part attributed to the *in vivo* data being obtained on a different panel of human subjects and to the administered dosage being 0.84 times that of the others. This result exemplified the general inability of *in vitro* testing to predict differences in extents of bioavailability that are likely attributable to specific biological mechanisms whose operation was relatively insignificant or absent in contributing to the bioavailability behavior of other dosage forms for which relatively accurate predictions or correlations are observed.

Systematically optimized *in vitro* dissolution testing conditions based on the ability of the test to predict *in vivo* drug response behavior (3) are recommended whenever practical. Alternatively, an approach to continuously upgrading the reliability and applicability of the transfer function used to predict *in vivo* drug product response curves computationally from the results of commonly employed testing methodologies is suggested. However, the usefulness of the described approach remains to be demonstrated in actual practice.

APPENDIX: ANALOG COMPUTER METHOD FOR CONVOLUTION AND DECONVOLUTION

The operations of deconvolution (Eq. 6) and convolution (Eq. 7) can be performed with an analog computer. Although curve fitting can also be done with an analog computer, it can most readily be accomplished with a digital computer using programs such as MULTIFIT (19), MBDX-85, or PLTEST (17) to obtain a multiexponential fit of observed *in vitro* data points to:

$$Q_D(t)_r = \sum_{1=i}^{n} A_i e^{-m_i t} \qquad \text{(Eq. A1)}$$

The A_i and m_i equation parameters are then used to set the potentiometers in an analog computer circuit, which is appropriate for performing deconvolution. An analog electrical signal representing the $G_B(t)_r$ function, against which $Q_D(t)_r$ is to be deconvolved to obtain $G_{DB}(t)_r$, can be produced using a variable diode function generator. Alternatively, $G_{DB}(t)$ can be obtained directly on a digital computer using the PLTEST program (17, 23). The PLTEST program, as developed in this laboratory, is recommended because it will accept properly interpolated $Q_D(t)_r$ and $Q_B(t)_r$ observed data and perform their deconvolution to provide $Q_{DB}(t)_r$ in the form of a multiexponential expression, which it derives from curve fitting a Bode diagram generated by the program.

The analog computer approach for performing convolution described here can be modified to accomplish deconvolution, as will be shown later. However, convolution is required to obtain $Q_B(t)_i$ by convolving $Q_D(t)_i$ against $G_{DB}(t)_r$, which has been fitted with a sum of exponentials expression. The approach is developed for biexponential fits to $G_{DB}(t)_r$ [*i.e.*, $G_{DB}(t)_r = A_i e^{-m_i t} + A_2 e^{-m_2 t}$]. A similar derivation for third- or higher order systems does not involve any new principles.

For a second-order system, the ratio of biological plasma level output to *in vitro* dissolution input is given in the Laplace domain by Eqs. A2–A4 for an ith dosage form:

$$\frac{Q_B(s)_i}{Q_D(s)_i} = G_{DB}(s)_r \qquad \text{(Eq. A2)}$$

$$\frac{Q_B(s)_i}{Q_D(s)_i} = \frac{A_1}{m_1 + s} + \frac{A_2}{m_2 + s} \qquad \text{(Eq. A3)}$$

$$\frac{Q_B(s)_i}{Q_D(s)_i} = \frac{A_1 m_1 + A_2 m_2 + (A_1 + A_2)s}{s^2 + (m_1 + m_2)s + (m_1 m_2)} \qquad \text{(Eq. A4)}$$

Dividing the numerator and denominator by s^2 and substituting $\alpha = A_1 m_1 + A_2 m_2$ into Eq. A4 yield:

$$\frac{Q_B(s)_i}{Q_D(s)_i} = \frac{(A_1 + A_2)s^{-1} + \alpha s^{-2}}{1 + (m_1 + m_2)s^{-1} + (m_1 m_2)s^{-2}} \qquad \text{(Eq. A5)}$$

A variable, $R(s)$, is now defined by Eqs. A6 and A7:

$$R(s) = \frac{Q_D(s)_i}{1 + (m_1 + m_2)s^{-1} + (m_1 m_2)s^{-2}} \qquad \text{(Eq. A6)}$$

$$R(s) = \frac{Q_B(s)}{(A_1 + A_2)s^{-1} + \alpha s^{-2}} \qquad \text{(Eq. A7)}$$

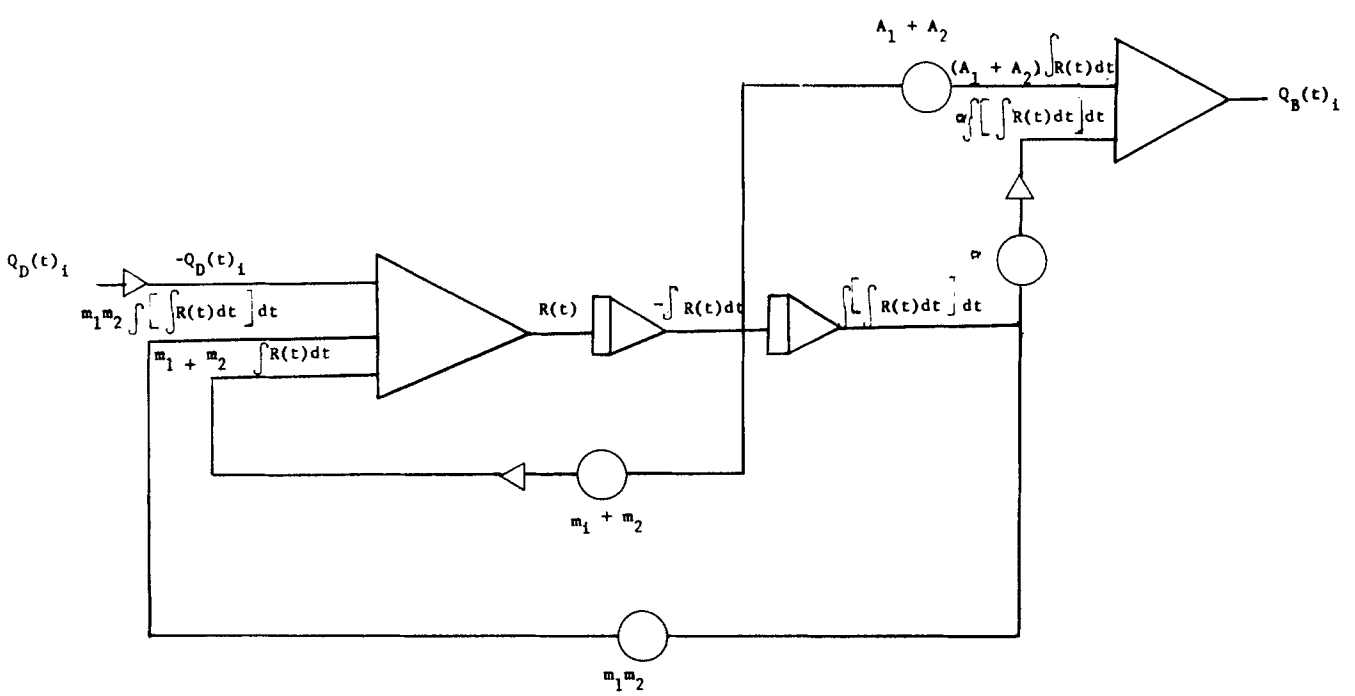

Figure 9—*Circuit diagram showing solution of Eq. A11 to give* $Q_B(t)$, *using* R(t) *and its integrals.*

Equations A6 and A7 are rearranged to yield Eqs. A8 and A10 in the Laplace domain and Eqs. A9 and A11 in the time domain:

$$R(s) = Q_D(s)_i - (m_1 + m_2)s^{-1}R(s) - (m_1m_2)s^{-2}R(s) \quad \text{(Eq. A8)}$$

$$R(t) = Q_D(t)_i - (m_1 + m_2)\int R(t)\,dt - m_1m_2\int [\int R(t)\,dt]\,dt \quad \text{(Eq. A9)}$$

$$Q_B(s)_i = (A_1 + A_2)s^{-1}R(s) + \alpha s^{-2}R(s) \quad \text{(Eq. A10)}$$

$$Q_B(t)_i = (A_1 + A_2)\int R(t) + \alpha\int [\int R(t)\,dt]\,dt \quad \text{(Eq. A11)}$$

Equation A9 is solved on the analog computer to give $R(t)$; Eq. A11 is then solved to give $Q_B(t)$ using $R(t)$ and its integrals as shown by the circuit diagram in Fig. 9.

A similar approach can be applied to solve for input functions by rearranging Eqs. A6 and A7 to give $R(s)$ and the input function and solving these on the analog computer. Therefore, both convolution and deconvolution can be performed by this general approach which, when modified in this manner, can also be used to deconvolve $Q_D(t)_r$ against $Q_B(t)_r$ to obtain $G_{DB}(t)_r$.

REFERENCES

(1) S. A. Kaplan, in "Dissolution Technology," L. F. Leeson and J. T. Carstensen, Eds., APhA Academy of Pharmaceutical Sciences, Washington, D.C., 1974, pp. 163–187.

(2) V. F. Smolen, P. B. Kuehn, and E. J. Williams, *Drug Develop. Commun.*, **2**, 143 (1975).

(3) V. F. Smolen and W. A. Weigand, *J. Pharm. Sci.*, **65**, 1718 (1976).

(4) V. F. Smolen, *ibid.*, **60**, 878 (1971).

(5) V. F. Smolen, *Hosp. Pharm.*, **4**, 14 (1969).

(6) W. Brownell, S. Riegelman, and W. J. Mader, "Committee Report on Drug Dissolution Methodology," APhA Academy of Pharmaceutical Sciences, Washington, D.C., 1968.

(7) G. Levy and L. E. Hollister, *J. Pharm. Sci.*, **58**, 1368 (1969).

(8) G. Levy, *ibid.*, **52**, 1039 (1963).

(9) M. Gibaldi and H. Weintraub, *ibid.*, **58**, 1368 (1969).

(10) H. Weintraub and M. Gibaldi, *ibid.*, **59**, 1792 (1970).

(11) J. G. Wagner, P. G. Welling, P. L. Kwang, and I. E. Walker, *ibid.*, **60**, 666 (1971).

(12) W. A. Cressman, C. A. Janicki, P. C. Johnson, J. T. Doluisio, and G. A. Braun, *ibid.*, **58**, 1516 (1969).

(13) V. F. Smolen, *J. Pharmacokinet. Biopharm.*, **4**, 337 (1976).

(14) *Ibid.*, **4**, 355 (1976).

(15) D. S. Riggs, "Control Theory and Physiological Feedback Mechanisms," Williams & Wilkins, Baltimore, Md., 1970, pp. 23–26.

(16) *Ibid.*, pp. 91–97.

(17) E. R. Rodeman and J. T. P. Yao, "Structural Identification—Literature Review," NSF Technical Report Ce-STR-73-3, School of Civil Engineering, Purdue University, West Lafayette, Ind., 1973.

(18) C. D. McGillem and G. R. Cooper, "Continuous and Discrete Signal and System Analysis," preliminary ed., School of Electrical Engineering, Purdue University, West Lafayette, Ind., 1971, pp. 6–1 ff.

(19) R. D. Schoenwald, Ph.D. thesis, Purdue University, West Lafayette, Ind., 1971, p. 313.

(20) M. Pernarowski, in "Dissolution Technology," L. F. Leeson and J. T. Carstensen, Eds., APhA, Academy of Pharmaceutical Sciences, Washington, D.C., 1974, pp. 58–105.

(21) C. D. McGillem and G. R. Cooper, "Continuous and Discrete Signal and System Analysis," preliminary ed., School of Electrical Engineering, Purdue University, West Lafayette, Ind., 1971, pp. 3–43 ff.

(22) V. F. Smolen, E. J. Williams, and P. B. Kuehn, *Can. J. Pharm. Sci.*, **10**, 95 (1975).

(23) P. B. Kuehn, Ph.D. thesis, Purdue University, West Lafayette, Ind., 1974.

ACKNOWLEDGMENTS AND ADDRESSES

Received March 12, 1976, from the *Interdisciplinary Drug Engineering and Assessment Laboratory and the Department of Industrial and Physical Pharmacy, School of Pharmacy and Pharmacal Sciences, Purdue University, West Lafayette, IN 47907.*

Accepted for publication May 4, 1976.

[x] To whom inquiries should be directed.

Pattern Recognition II: Investigation of Structure–Activity Relationships

GOVIND K. MENON and ARTHUR CAMMARATA [x]

Abstract □ A simple form of pattern recognition is successfully used to classify a set of structurally diverse therapeutic agents. By using only organic structural information, the major pharmacological classes present were correctly identified and the pharmacologically unrelated compounds were separated out. One technique of factor analysis—principal component analysis—is shown to be readily adaptable in preprocessing the data. Simple graphical representation of the results enables their direct interpretation.

Keyphrases □ Structure–activity relationships—determined using pattern recognition methods of analysis, various drugs □ Pattern recognition—analysis methods used to determine therapeutic classes of various drugs □ Factor analysis techniques—used to determine therapeutic classes of various drugs

The application of pattern recognition methods in solving chemical problems has provided the incentive for considerable research within the past few years (1–6). Recently, these methods have been applied in the development of new biological agents due to their capacity to analyze rapidly large stores of accumulated information and to detect substances worthy of further investigation (7–10). In other words, the techniques can be directed toward establishing structural specificity in biological action, providing rationales in selecting substances for biological assay, and identifying pharmacophoric patterns of molecular substitution (1).

Several detailed accounts describe the various pattern recognition techniques (11–14), but a brief conceptual summary follows. Pattern recognition involves the detection and recognition of regularities or invariant properties among accumulated (often large) sets of measurements, the purpose being to provide a basis for new hypotheses. For example, consider an attempt to derive a